Metric and non-metric guides for the determination between fore- and hindlimb phalanges of *Rangifer tarandus*

Emily H. Hull

Department of Anthropology, University of Alberta, 13-15 Tory Building, Edmonton, Alberta, Canada T6G 2H4 (Corresponding author: ehull@ualberta.ca).

Abstract: Phalanges are a great untapped resource in the zooarchaeology of *Rangifer tarandus*. The utilization of this resource, however, is constrained by a current inability to consistently differentiate fore- from hindlimb phalanges in a mixed assemblage. The ability to separate and identify forelimb and hindlimb phalanx 1 (PI) and phalanx 2 (PII), as well as to recognize and identify other small bones of the hoof, leads to great opportunities for archaeologists. In large-scale analysis, this capacity allows a greater ability to determine minimum number of individuals and assess butchery and transport practices. In the examination of individual life histories of *Rangifer tarandus*, these designations allow a more precise study of pathology and entheseal change, which can shed light on adaptation, foraging strategy, and human-animal interactions. This study presents qualitative and quantitative methods for the differentiation of PI and PII of the fore- and hindlimbs and describes other bones of the hoof. Metric techniques were developed to differentiate fore- from hindlimb phalanges using non-invasive, non-destructive, and simple methods. The efficacy and accuracy of these methods were assessed using blind testing by students and staff. The average success rates of metric analysis yielded 87% accuracy for determinations of fore- versus hindlimb PI and 92% accuracy for determination of fore- versus hindlimb PII. These results show that this method could benefit researchers working with *Rangifer tarandus* remains.

Key words: metacarpal; metatarsal; osteometrics; osteology; phalanges; *Rangifer tarandus*; zooarchaeology.

Rangifer, 39, (1), 2019: 11-26
DOI 10.7557/2.39.1.4630

Introduction

Zooarchaeological relevance of phalanges

While often ignored due to their small size and difficulty in assessment, phalanges are nonetheless an untapped resource available to zooarchaeologists studying ungulates in general and *Rangifer tarandus* in particular. Because most cervid bones are broken or dispersed in archaeological deposits, either by human processing or by subsequent animal scavenging, intact skulls, long bones, or pieces of the axial skeleton are not commonly recovered. By contrast, the hooves, which have minimal meat, contain a network of tough tendinous and cartilaginous tissues, and are therefore less enticing for butchering or scavenging. Bones of the hoof are dense, small, and strong, and thus more often intact. In fact, whole phalanges are commonly found in human-kill and butchering deposits (Binford, 1981). Important osteometric studies of animal phalanges have been performed, especially in Bovids. These can be seen in the

designation between fore- and hind-limb cattle phalanges (Dottrens, 1946), the use of phalanges in sex determination of bison (Duffield, 1973), and the subsequent study of metrics and paleopathology in the phalanges of cattle (Bartosiewicz, 1993; Bartosiewicz *et al.*, 1993). Cervids, however, have not been the subject of such studies, perhaps because *Rangifer tarandus* is the only domesticated cervid. This study describes both qualitative and quantitative methods for the study and distinction of *Rangifer tarandus* phalanges.

In zooarchaeological quantification, phalanges of *Rangifer* are often lumped together, with no attempts to divide fore- and hindlimb phalanges. The extreme difficulty in separating phalanges, due to similarities in morphology and size, may lead to the belief that phalanges of the fore- and hindlimb cannot be differentiated.

Separating both phalanx 1 (PI) and phalanx 2 (PII) of the fore- from hindlimb is significant to both assemblage-based analyses and individual life history studies in zooarchaeology. As phalanges are often among the most abundant complete bones in archaeological *Rangifer tarandus* assemblages, they offer a wealth of information. In assemblage-based analysis, more precise calculations of minimum number of individuals (MNI) are made possible by the specific identification of phalanges. For example, an assemblage with 400 first phalanges, assessed together without designations, must be initially considered to have an MNI of 50, as each individual *Rangifer tarandus* possesses 8 such elements. With more detailed assessment, MNI values can become much more precise. Further, the ratio of fore- to hindlimb phalanges may also give information as to human utilization, butchery practices, and preferential meat procurement (Binford, 1961; Binford, 1978; Steele, 2015). Identifying phalanges is also useful for analyses of *Rangifer* life histories. Different pathologies of fore- and hindlimb phalanges, as well as differences in entheseal changes at muscle attachment sites, may tell archaeologists much about the behavioral patterns of individual animals in life (Bartosiewicz & Gál**,** 2013; Villotte & Knüsel, 2013; Niinimäki & Salmi, 2016; Salmi & Niinimäki, 2016).

Background

Rangifer tarandus is a circumpolar and medium-sized cervid species with large hooves (Banfield, 1961). They are artiodactyls with cloven hooves and large dewclaws that often function as additional, rather than vestigial, toes. Their pattern of morphology follows that of the Telemetacarpalia, a subgroup of Cervidae. In this morphological adaptation, metacarpal (MC) I is not present, and metacarpals III and IV are fused into the central metapodial. Metacarpals II and V are foreshortened to become the dewclaws, which each include a vestigial metacarpal bone, and small PI, PII, and PIII, as well as a small sesamoid bone. In the metatarsal (MT), an analogous development is present, in which the vestigial metatarsals II and V are absent, leaving only the small PI, PII, and PIII, and small sesamoid bone. Metatarsals III and IV are fused into a single metatarsal (Nieminen, 1980, Nieminen, 1994; Cap *et al.*, 2002).

The unique morphology of *Rangifer tarandus* is epitomized by the size of the feet, much of which is due to the dish-shaped cartilage which covers PIII and appears, in living animals, as the hoof. Telfer & Kelsall (1984) found that *Rangifer tarandus* hoof-to-body-size ratio is more similar to the paw-size of North American predators than to the hoof-size of other cervids. This may be due to their cold-weather adaptation, and again indicates that their morphology must be studied separately and not determined from proxy studies of other artiodactyls (Formozov, 1946; Nieminen, 1994; Geist, 1998).

Materials and Methods

Forty modern skeletal specimens from Finland housed at the University of Oulu were visually inspected. The collections contained both *Rangifer tarandus tarandus* and *Rangifer tarandus fennicus* of both sexes, all of which were skeletally mature. All had phalanges labelled by side and limb, and these were used in equation design and testing. In addition, six hooves belonging to domestic *Rangifer tarandus tarandus* were dissected for the study. The blind testing was done with a wider range of subspecies, including specimens of *Rangifer tarandus fennicus, Rangifer tarandus tarandus*, and *Rangifer tarandus caribou* from collections at both the University of Oulu and the University of Alberta, Canada. Each test was completed by 23-25 volunteers (dependent upon the test and the time volunteers had available). Volunteers for the blind test were all staff and students at the University of Oulu and the University of Alberta. The volunteers were comprised of 18 students with limited osteological experience, and 7 graduate students and staff with experience in osteology or zooarchaeology. Tests were discarded only for two reasons: first, in one case, improper use of the calipers led to measurements that were up to 220 mm larger than those found by their peers, or, second, the volunteer had written their name or other identification on the test. All tests were given in accordance to ethics approval by the University of Alberta.

Initially, to develop specific written and illustrated descriptions of each bone that could be used to aid in siding and land-marking, each phalanx was examined in detail, and a representative description and diagram highlighting its anatomy and the differences between elements was produced (Fig.2).

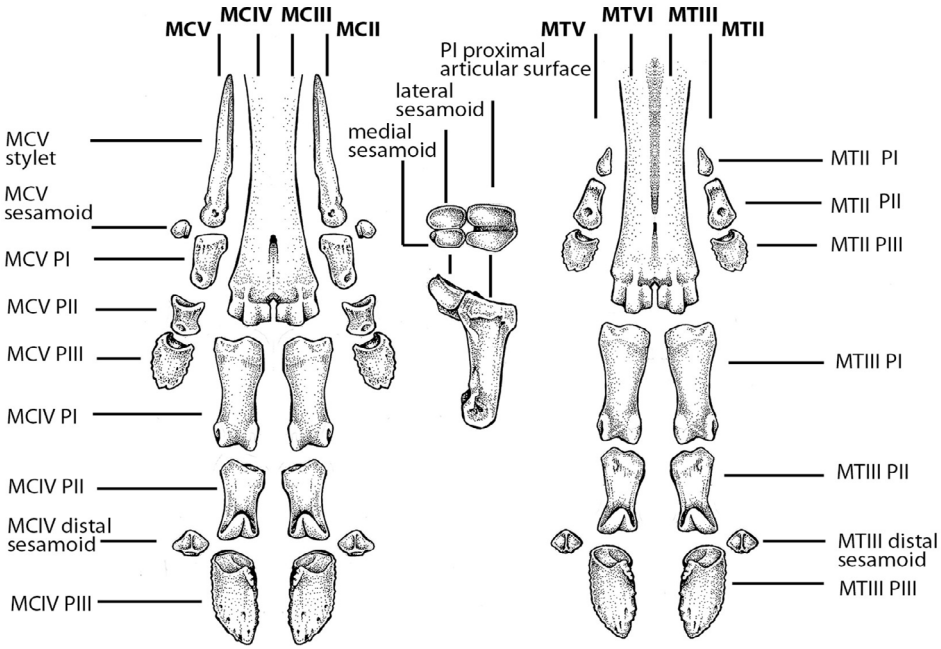

Figure 1. Metapodials, phalanges, and dewclaws, designated by metacarpal/metatarsal and phalanx number. Forelimb is pictured on the left and hindlimb on the right, with proximal sesamoids depicted in the center. (Both illustrations depict right limbs, although it should be noted that at this time there is no accurate test for determining right-limb from left-limb phalanges). Illustration by author.

Secondly, equations were devised systematically distinguish PI and PII from those of the hindlimb. The primary measurements were adapted from those described for the measurement of long bones by von den Driesch (1976) but were supplemented with other measurements to capture more variation of shape observed. Equations were derived and tested based on each phalanx's most distinct, definitive, and consistent morphological features. Six measurements were taken on each PI, and twelve on each PII, based on the most distinctive features of the bone. More measurements were taken on PII because of their extreme difficulty to separate visually. An additional goal was to ensure that the resulting equations were simple, straightforward, and require no mensuration that could not be expediently achieved with calipers and a calculator. To this end, no more than four measurements were eventually selected for each equation. The overall objective was simplicity and utility in an archaeological context. While both osteometric and morphological techniques are presented in this study, it is hoped that these techniques may be used in conjunction, as visual assessments by morphology are intrinsically subjective, while osteometric techniques are more reliable.

Measurements were collected in a spreadsheet, and trial and error equations, developed with consideration to shape dynamics, were used to find the greatest degree of separation in results. Initial results were also analyzed for differences between the sexes, however, all differences were found to be in size, not in shape. The size difference also included significant overlap, so was deemed unreliable for sexing without additional context.

General anatomy of the phalanges

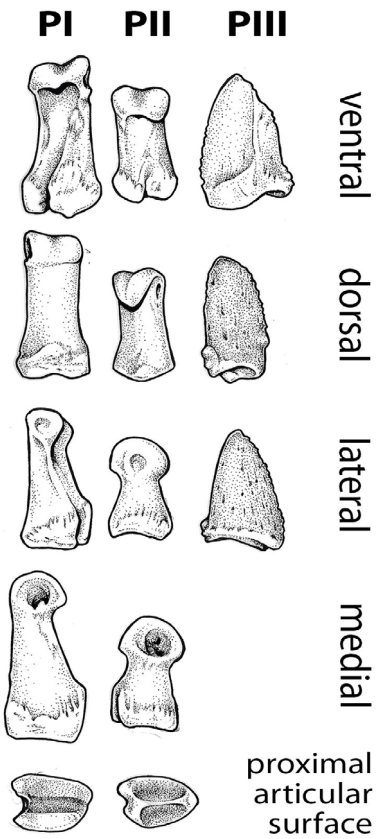

Figure 2. PI, PII, and PIII depicted from multiple angles, in reverse anatomical position. As each hoof contains two digits, and as the differentiation between the analogous digit of the opposite hoof cannot yet be quantified, each hoof will be presented as the entire subject of study, rather than the entire body of the animal. For this reason, it is important to clarify directional terminology. Medial and lateral sides are designated as medial and lateral to the center of the hoof, not to the animal's body. Thus, the medial side of a phalanx would be the side that faces the center of the hoof, towards the other digit of the same hoof. (Both illustrations depict right limb bones, although it should be noted that at this time there is no accurate test for determining right-limb from left-limb phalanges). Illustration by author.

Phalangeal anatomy may be divided into four sections (Fig. 1): Phalanges I and II, PIII (or the terminal phalanx), sesamoids, and bones of the dewclaws.

Phalanges I and II

While very different in detail, PI and PII follow a general morphological form. These phalanges consist of a distally-oriented head, diaphyseal body, and a concave, proximal articular base.

While it may seem obvious to more experienced zooarchaeologists, it is important to differentiate PI from PII, as this may not be clear to novices (Fig.2). PII is a much shorter, smaller bone than PI, and can be identified by the heart shaped profile of its head when observed from the distal aspect. While the shape of the distal articular surface on PI resembles a spool or a bow with two rounded articular condyles separated by a central groove, the heart-shaped profile of PII is formed by two condyles, again separated by a central groove, which meet at a rounded point on the dorsal side of the phalanx. On the proximal articular surface, PI has a generally rectangular surface, with a central sulcus running dorsally to ventrally, while PII's proximal articular surface is again an inverted heart-shape, with a central ridge running from a small flat surface (often with vascular foramina) at the ventral aspect of the articular surface; this runs through the length of the articular surface before curling upwards to a pointed protuberance on the dorsal side of the phalanx. This surface articulates with the spool-shaped distal articular surface of PI.

Differentiating medial from lateral sides of PI

On the distal articular surface of PI are two articular condyles (Fig. 3). One condyle is higher and has a steeper angle than the other. This condyle also typically has much more development on the tendon attachment site just proximal to the articular condyle on the side of the phalanx. This condyle marks the medial side of the phalanx, facing the centerline of the hoof. Additionally, on the proximal articular surface, the medial articular facet is broader and deeper than the lateral articular facet, which often appears as a slightly raised platform.

Differentiating medial from lateral sides of PII

On the distal articular surface of PII are two circular, concave areas just proximal to the distal articular surface on the sides of the bone. The more distinct, concave area marks the medial side of the phalanx. The lateral side will often be quite smooth, with minor or indistinct concavity (Fig. 4). Additionally, on the ventral aspect of the proximal articular surface are two protuberances divided by the central ridge bisecting the articular surface. The side with the longer dorsal to ventral length is the lateral side. This projection will also be generally more robust and protuberant than the medial side.

Differentiating fore- and hindlimb PI

In the same individual, forelimb PI may be distinguished as consistently shorter in length with a more robust base than hindlimb PI, which have a noticeably longer diaphysis (Fig. 3). While the distal articular condyles are quite analogous between the fore- and hindlimb, the proximal articular surfaces at the base of the phalanges are a key distinguishing feature. When viewed from the proximal aspect, directly at the articular surface with the metapodial, the base of forelimb PI is roughly square or circular, with generally equal length and breadth. By contrast, the medial articular facet of hindlimb PI includes a styloid-like protuberance, which extends along the length of the medial articular surface significantly farther than the lateral surface. While the medial articular facet of forelimb PI is often slightly longer than the lateral facet, this difference is not so different to obscure the squared or circular shape of the proximal articular surface of the forelimb phalanx. In the hindlimb PI, the entire articu-

lar surface is rectangular, extending much more significantly ventrally-to-dorsally than medially-to-laterally.

In PI, the most diagnostic differences in measurement were found to be the ratio between overall length and breadth of the base. Visual inspection revealed that the shape of the PI base is most representative, with forelimb PI being square-shaped and hindlimb PI being more rectangular. This visual difference was backed up by measurement of the longest length and breadth of the proximal articular surface.

Overall, the difference between fore- and hindlimb PI can be assessed by examining the ratio of width to breadth of the proximal articular surface (Fig. 3). In forelimb PI, the ratio of breadth to width will be equal to or greater than one, and in hindlimb PI, this ratio will be less than one. The most reliable method of differentiation was found in the equation (Appendix, Fig. I): A/B = X, where A = the breadth of the proximal articular surface, and B = the longest length of the proximal articular surface. When X ≥ 1, the phalanx is thoracic (forelimb), and when X < 1, the phalanx is pelvic (hindlimb). No results between 0.94 and 1.00 were recorded during the initial development of the equation (Fig.5).

Differentiating fore- and hindlimb PII

The difference between fore- and hindlimb PII

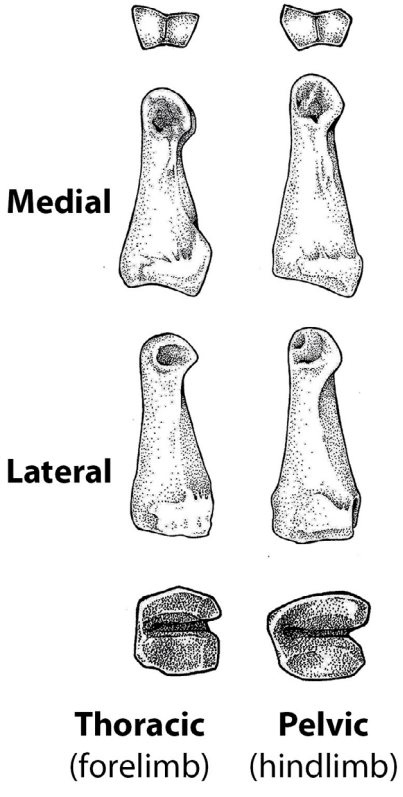

Figure 3. PI (Reverse anatomical position). Illustration by author.

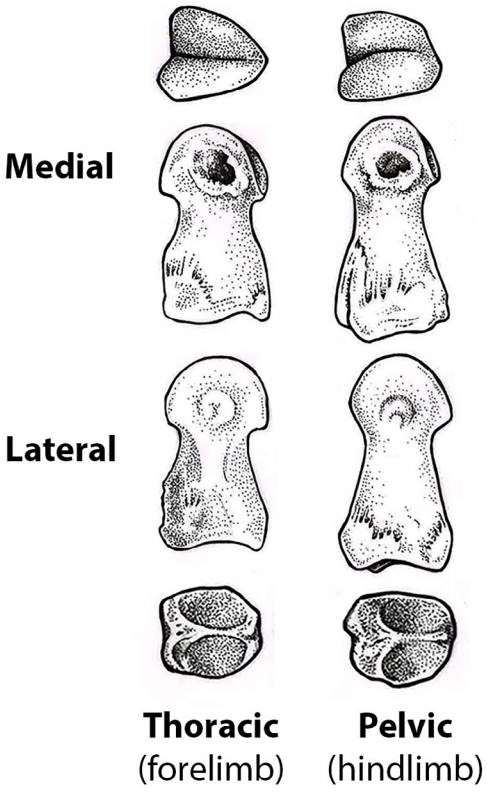

Figure 4. PII (Reverse anatomical position). Illustration by author.

in the same animal is subtle. If a single animal is present, the fore- and hindlimb PII can be sorted by general size and robusticity of several features (Fig.4). A forelimb PII is a shorter, more robust bone than a hindlimb PII. In both bones, the head of bone pinches in to create a neck at the distal end of the diaphysis before flaring out to a broad, heart-shaped base. The degree of constriction at this neck is much greater in a hindlimb PII than in a forelimb PII. An additional difference is the presence of more pronounced sharpness at the distal dorsal articular surface on a hindlimb PII, when the head of the phalanx is viewed from the side.

When analyzing disarticulated remains of incomplete or multiple animals, visual observation is not adequate to accurately separate the fore- and hindlimbs. There is significant overlap in the morphology in fore- PII and hindlimb PII from multiple individuals, especially those of different size, sex, and robusticity. For this reason, it is more reliable to use a metric system for analysis, especially for large numbers of individuals.

Several equations were tried using a multitude of variables (Appendix Fig. II), but the most consistent in separating fore- from hindlimb was (A+B)/C =X, where A= the longest total length, B= the length of the phalangeal base, and C= the smallest breadth of the neck. If X > 4.50, the phalanx is thoracic (forelimb); if X < 4.50, the phalanx is pelvic (hindlimb). No results between 4.45 and 4.55 were recorded during the initial development of the equation (Fig.6).

Anatomy and siding of PIII

In an individual animal, forelimb PIII may be differentiated from hindlimb PIII by its larger size (Fig.1). No reliable method has yet been found to differentiate fore- from hindlimb in a mixed-individual sample, and therefore must be the subject of further study. Siding, however, is quite clear. PIII is triangular in shape, with a proximal articular surface with three articular facets, and three generally flat surfaces converging to a pointed distal end. The largest, most curved of these surfaces forms the dorsal side of

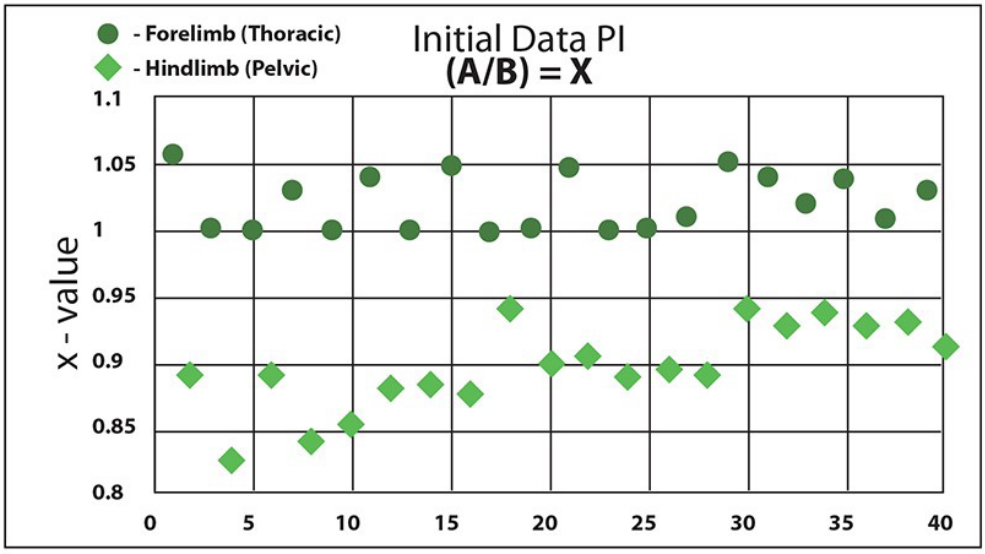

Figure 5. PI. Graph of values from the initial sample (n=40).

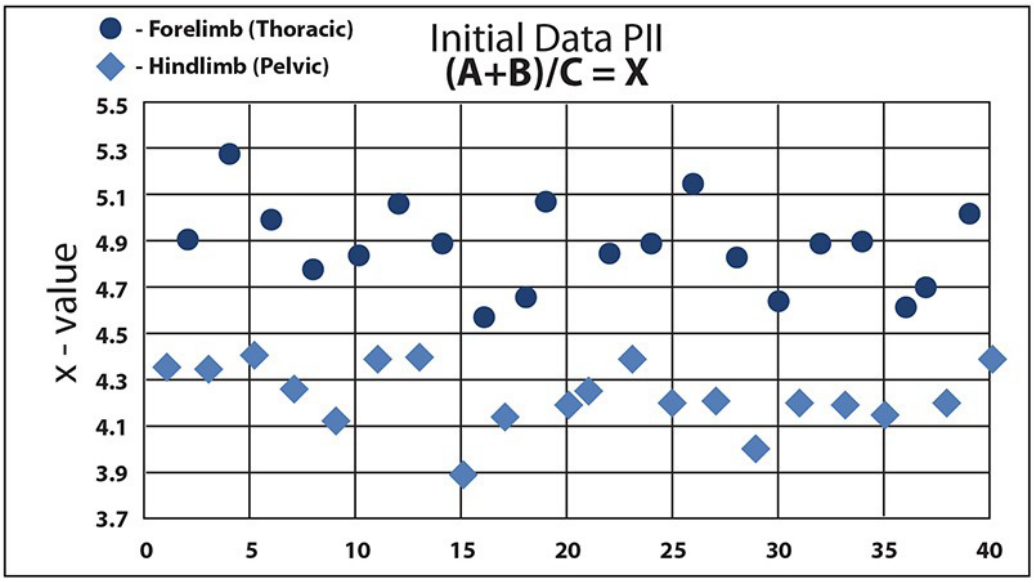

Figure 6. PII. Graph of values from the initial sample (n=40).

the hoof and can be additionally recognized by its high degree of ruggedness and plethora of vascular foramina. The ventral surface of PIII is quite smooth and often only shows ruggedness along muscle attachment sites at the proximal border and along the lateral edge of the surface. The medial surface of PIII is the smallest of the three sides, and houses two large vascular foramina just distal to the articular surface. The largest of these is present along the ventral edge of the surface. In order to side PIII, simply place it on the table in anatomical position, and the position of the medial surface will show whether it is on the medial or lateral side of the hoof. The two largest articular facets articulate with the head of PII. The smallest, on the most dorsal aspect of the articular surface, articulates with the distal sesamoid bone. This articular facet is also distinct between the fore- and hindlimb of the same individual, with the forelimb PIII's sesamoid articular facet being both smaller and more medially located than that of hindlimb PIII. Because of the range of inter-individual variation, however, neither this criteria nor size can be consistently used to separate fore- from hindlimb bones in a mixed assemblage.

Anatomy of the sesamoids

Proximal sesamoids

Two proximal sesamoids (Fig.1) attach to the proximal dorsal aspect of PI and articulate with both the metapodials and PI in both the fore- and hind-limb. They can easily be differentiated into medial and lateral by their distinct shape. They are both lunate in shape, but the ventral, non-articular surface of the medial sesamoid is much more rounded. By contrast, the ventral, non-articular aspect of the lateral sesamoid extends to a rounded ridge. While the medial sesamoid is ovoid in shape with a flat base, the lateral appears more as a medially-to-laterally flattened trapezoid. The difference in morphology of these bones is consistent enough to be used to distinguish these bones in a mixed assemblage.

Dorsomedial sesamoid

The most overlooked bone in the hoof is a small, flat, and circular bone embedded in

the extensor tendons of the front hooves. The dorsomedial sesamoid is located dorsally at the joint between PI and PII on the forelimbs. At this junction, it acts analogously to a miniature patella, but more study is needed to understand its full function and development.

Distal/navicular sesamoid

The distal sesamoid bone makes up the heel of the hoof. It articulates with PIII on the proximal dorsal aspect and can be identified by its unique shape. This bone is shaped differently in the fore- and hindlimb hooves. The forelimb distal sesamoid is small and has the general shape of an equilateral triangle, with two dorsal articular facets of equal size articulating with PII. A round articulation at the distal end, at the opposite face from the apex of its triangular shape, articulates with PIII.

In the hindlimb, the distal sesamoid bone is larger, with uneven articular facets; the lateral facet has a larger surface area and creates the general shape of an obtuse triangle. Like the distal sesamoid of the forelimb, it has three articular facets in the same configuration: two articulating with PII, and one articulating with PIII. Despite these disparities, inter-individual variation makes these differences inappropriate for the determination of fore- from hindlimb phalanges in a multi-individual setting.

Dewclaws

Dewclaws of *Rangifer tarandus* (Fig. 2) contain their own unique skeletal anatomy, analogous to but distinct from the primary metapodials and digits of the hoof. They do not directly articulate at any point with the metapodial but are instead held in place by a network of connective tissue and ligaments. The forelimb dewclaws contain vestigial MCII and MCV which appear as sharp, linear stylet with a rounded distal articular surface (Barone, 1986). At this point, a rudimentary PI, PII, and PIII all articulate in succession beginning with the MCII/MCV and MCIIPI/MCVPI. In hindlimb dewclaws, the MCII/MCV stylet component is no longer present, and the complex contains only the phalangeal bones of MCIIPI/MCVPI, MCIIPII/MCVPII, and MCIIPIII/MCVPIII.

Differentiation between primary PIII and dewclaw PIII

The bones of the dewclaw are unlikely to be mistaken for any other bones of the hoof with one exception: PIII. While size is an important distinguishing factor between the PIII of the dewclaws and the primary PIII bones, it is important to note morphological differences, as the dewclaw PIII bones of a large adult animal may be close in size to the primary PIII bones of a small, young animal. Morphologically, PIII of the dewclaws have rough, vascularized edges around the entire border of the bone apart from the proximal articular surface, and is bifacial, having a front and a back surface running the length of the bone. By contrast, primary PIII bones have a triangular shape and have a rough, serrated edge only on the external margin. The internal border of the dewclaw PIII is smooth, straight, and flat, emerging nearly perpendicularly from the dorsal surface. Both PIII bones have large vascular foramina, which occurs on the dorsal surface of the dewclaw PIII and the interior surface of primary PIII bones.

Blind tests

Students all used digital calipers to diminish errors that might be made while reading traditional dial calipers. Each bone was marked with a number or letter on tape, which also covered their collection specimen numbers, as these could have provided bias to the experienced osteologists.

Test A: Qualitative test

Volunteers (n=25) were given ten randomly numbered PI and PII phalanges with red and blue dots randomly placed on the sides of each.

They were asked to use the diagrams (Fig. 3 and 4) and the descriptions above to designate them as PI and PII as well as to identify the medial and lateral sides of each bone. The purpose of this test was two-fold: first, to assess the usefulness of the illustrated guide and descriptions, and second, to allow the novice volunteers to become more comfortable observing the phalanges.

Test B: Qualitative and quantitative differentiation between forelimb (TPI) and hindlimb (PPI) (Appendix; Fig. I)

Volunteers (n=23) were given a randomly numbered sample of ten PI phalanges and assigned (in separate sub-tests) to use illustrations and diagrams (provided in the Appendix) to divide them into fore- and hindlimb bones first, and then to use equations to do the same. This was done to compare the effectiveness of observation versus quantitative analysis.

Test C: Qualitative and quantitative differentiation between forelimb (TPII) and hindlimb (PPII) (Appendix; Fig. II)

Volunteers (n=23) were given a randomly numbered sample of ten PII phalanges and asked (in separate sub-tests) to use illustrations and diagrams (provided in the Appendix) to divide them into fore- and hindlimb bones first, and then to use equations to do the same. This was done to compare the effectiveness of observation versus quantitative analysis.

Results

Projected test results

It was expected that the Test A would produce consistently good results, as the differences between PI and PII, and medial and lateral aspects were quite distinct once identified. It was projected that Test B, differentiating fore- and hindlimb PI, would result in a high rate of correct assessments as the equation is quite simple and the differences between the elements are often observable to the eye. It was thought that Test C would produce a lower rate of correct assessments, as the differences are very subtle to observe and the equation involves somewhat more complex measurements.

Blind test results

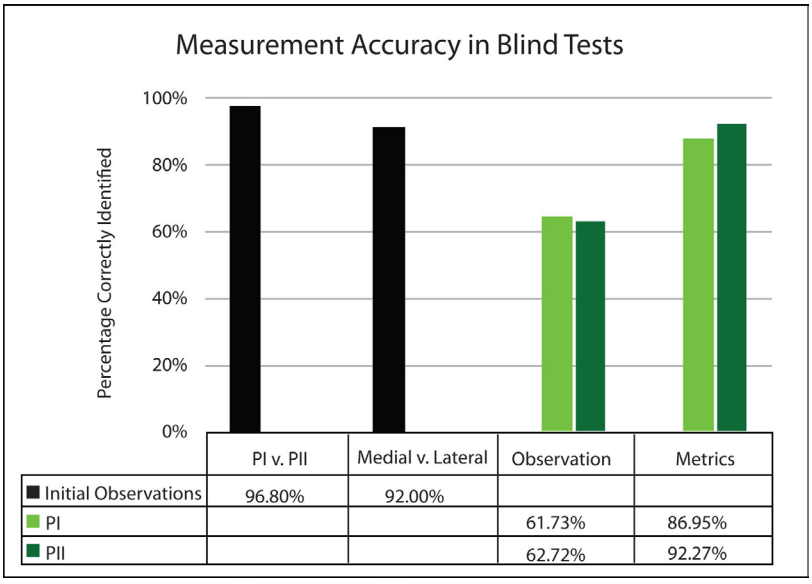

Figure 7. Graph of blind test results. Black bars represent Test A; light green, PI Test B; dark green, PII Test C.

Discussion

While the blind tests did support the higher accuracy of metric determinations versus observation, the projected comparative accuracies of each test were somewhat unexpected. Designation between PI and PII, as well as the determination of medial and lateral aspects were very consistent. Any errors may be explained by the inexperience of some of the volunteers. The unexpected results appear in the metric determination between PI and PII. Because of the simplicity and observability of fore- versus hindlimb PI, it was expected that both observation and metric tests of this digits would yield the highest accuracy. The actual results, however, belied this hypothesis (Fig.7). Results of observation were nearly indistinguishable between PI and PII (62% and 63%, respectively), and the PII metric blind tests yielded higher accuracy than the PI tests, with PII metric tests yielding a mean of 92% (mode= 100%) accuracy, and PI metric tests a mean of 87% (mode= 90%) accuracy. To check observer reliability, measurements from the volunteers were assessed by calculating Intraclass Correlation Coefficients. According to generally accepted standards, an Intraclass Correlation Coefficient (ICC) with a value over .750 is considered excellent, while an ICC value of between 0.60 and 0.74 is considered good (Cicchetti, 1993; Fleiss, 1986). In this study, the ICC values were calculated for absolute agreement between blind testers. The ICC for Test B showed an average measure value of .989. The ICC for Test C showed an average measure value of 1.000. All values are shown in Fig. 8.

There are multiple possible reasons for the discrepancy between measurement accuracy between PI and PII. First, perhaps a lack of familiarity with calipers led to minute measurement errors that became more apparent in the PI equation, which is a direct ratio, rather than in the PII equation, which is a more complex calculation. Second, as PI has a circumference-long area of rugosity and muscle attachment sites just distal to the edge of the articular surface (Fig. 1, Fig. 2), it is possible that the volunteers were measuring from this highly variable area, rather than from the edge of the articular surface. For this reason, the guidelines were amended to warn against this possibility. Another possible reason for the error margin is that participants may have paid more attention to the blind test with the more complex measurements, thereby giving this test more accuracy. The results, however, do support the usability and effectiveness of these measurement guidelines, especially with experience and practice.

PI:

	Intraclass Correlation	95% Confidence Interval	
		Lower Bound	Upper Bound
Single Measures	.827	.725	.913
Average Measures	.989	.980	.995

PII:

	Intraclass Correlation	95% Confidence Interval	
		Lower Bound	Upper Bound
Single Measures	.997	.995	.998
Average Measures	1.000	1.000	1.000

Figure 8. ICC values calculated for absolute agreement between blind testers.

Conclusions

While many current studies produce detailed results with advanced morphometrics, it was important in the design of this study to utilize simple measurements and to produce equations that could be done in the field or lab with only a set of calipers. The blind tests were done by students and staff who, with few exceptions, had never before studied or done metrics on *Rangifer tarandus* remains, and many had never practiced metrics analysis of any kind. The level of accuracy during their initial attempts suggests that with practice, accuracy would only increase. In the creation of these descriptions, diagrams, and equation-based determinations, the focus was on non-destructive usability, and this was demonstrated to be the case in the blind tests. With these guidelines and tools, more precise determination of fore- and hindlimb phalanges is clearly possible. Traditional zooarchaeology and assemblage-based analysis could utilize this technique for more precise determination of MNI, butchery practices, and preferential transport of meat. In studies of domestication, it has been shown that reindeer involved in different activities show different entheseal changes and pathologies; this technique could benefit this study by allowing the differential analysis of the habitual stressors on fore- versus hindlimb (Niinimäki & Salmi, 2016; Salmi & Niinimäki, 2016). Finally, in the emerging and expanding research areas of human-animal relationships, individual animal life histories, and animal ontologies, a more distinct understanding of the bones of the hooves may help elucidate topics from habitat, foraging techniques, and individual pathology. This technique has the potential to be an extra tool in the study of the osteology and archaeology of *Rangifer tarandus* in both modern and ancient America and Eurasia.

Acknowledgements

I would like to acknowledge the incredible support and guidance of Dr. Robert Losey of the University of Alberta, as well as Dr. Anna-Kaisa Salmi, Dr. Sirpa Niinimäki, and Hanna-Leena Puolakka of the University of Oulu. Invaluable assistance was provided by my research assistant, Mitchell Semeniuk. Additional thanks are due to all the wonderful volunteers who participated in testing the metrics and methodology.

References

Banfield, A. W. F. 1961. A revision of the reindeer and caribou genus Rangifer (No. 66). Ottawa: Queen's Printer.

Barone, R. 1986. *Anatomie Comparée des Mammifères Domestiques, tome 1, Ostéologie.* Paris: Vigot Freres.

Bartosiewicz, L. 1993. The anatomical position and metric traits of phalanges in cattle. — *Revue de Paléobiologie* 12(2):21-43.

Bartosiewicz, L., & Gál, E. 2013. *Shuffling Nags, Lame Ducks: The Archaeology of Animal Disease.* Oxford: Oxbow Books. https://doi.org/10.2307/j.ctvh1djdq

Bartosiewicz, L., Van Neer, W. and Lentacker, A. 1993. Metapodial asymmetry in draft cattle. — *International Journal of Osteoarchaeology* 3(2):69-75. https://doi.org/10.1002/oa.1390030203

Binford, L. R. 1977. *For theory building in archaeology: Essays on faunal remains, aquatic resources, spatial analysis, and systemic modeling*. New York: Academic Press.

Binford, L. R. 1978. *Nunamiut: Ethnoarchaeology*. New York: Academic Press.

Binford, L. R. 1981. *Bones: ancient men and modern myths.* New York: Academic Press.

Cap, H., Aulagnier, S., & Deleporte, P. 2002. The phylogeny and behaviour of Cervidae (Ruminantia Pecora). – *Ethology, Ecology, & Evolution* 14(3):199-216. https://doi.org/10.1080/08927014.2002.9522740

Cicchetti, D. V. 1994. "Guidelines, criteria, and rules of thumb for evaluating normed and standardized assessment instruments in psychology". — *Psychological Assessment* 6 (4):284–290. https://doi.org/10.1037//1040-3590.6.4.284

Dottrens, E. 1946. Étude préliminaire: les phalanges osseuses de *Bos taurus domesticus*. — *Rev. suisse de Zool* 53(33):739-774.

von den Driesch, A. 1976. *A guide to the measurement of animal bones from archaeological sites: as developed by the Institut für Palaeoanatomie, Domestikationsforschung und Geschichte der Tiermedizin of the University of Munich* (Vol. 1). Cambridge: Peabody Museum Press.

Duffield, L.F. 1973. Aging and sexing the post-cranial skeleton of bison. — *Plains Anthropologist* 18(60):132-139. https://doi.org/10.1080/2052546.1973.11908656

Fleiss, J.L. 1986. *The design and analysis of clinical experiments.* John Wiley & Sons, Inc.

Formozov, A. N. 1946. *Snow cover as an integral factor of the environment and its importance in the ecology of mammals and birds* (No. 1). Edmonton, Alberta: Boreal Institute, University of Alberta.

Geist, V. 1998. *Deer of the world: their evolution, behavior, and ecology*. Mechanicsburg, PA: Stackpole Books.

Nieminen, M. 1980. Evolution and taxonomy of the genus *Rangifer* in northern Europe. – *In:* Reimers, E., Gaare, E., and Skjenneberg, S. (Eds.). *Proceedings Second International Reindeer/Caribou Symposium.* Direktorate for vilt og ferskvannisfisk, Trondheim, Norway. pp. 379-391.

Nieminen, M. 1990. Hoof and foot loads for reindeer (Rangifer tarandus). — Rangifer 10(3):249-254. https://doi.org/10.7557/2.10.3.865

Nieminen, M. 1994. *Poro: ruumiinrakenne ja elintoiminnat*. Helsinki: Riista-ja kalatalouden tutkimuslaitos.

Niinimäki, S. and Salmi, A.K. 2016. Entheseal Changes in Free-Ranging Versus Zoo Reindeer - Observing Activity Status of Reindeer. — *International Journal of Osteoarchaeology* 26(2):314-323. https://doi.org/10.1002/oa.2423

Salmi, A.K. & Niinimäki, S. 2016. Entheseal changes and pathological lesions in draught reindeer skeletons – Four case studies from present-day Siberia. — *International Journal of Paleopathology* 14:91-99. https://doi.org/10.1016/j.ijpp.2016.05.012

Steele, T. E. 2015. The contributions of animal bones from archaeological sites: The past and future of zooarchaeology. — *Journal of Archaeological Science* 56:168-176. https://doi.org/10.1016/j.jas.2015.02.036

Telfer, E. S., & Kelsall, J. P. 1984. Adaptation of some large North American mammals for survival in snow. — *Ecology* 65(6):1828-1834. https://doi.org/10.2307/1937779

Villotte, S., & Knüsel, C. J. 2013. Understanding entheseal changes: definition and life course changes. — *International Journal of Osteoarchaeology* 23(2):135-146. https://doi.org/10.1002/oa.2289

Manuscript recieved 16 Jan 2019
revision accepted 5 June 2019
manuscript published 3 July 2019

Appendix

Guidelines for differentiation between fore and hindlimb PI and PII

For consistency and expedience, forelimbs were marked as "thoracic" limbs (TPI and TPII), and hindlimbs were marked as "pelvic" limbs (PPI and PPII).

Metric guidelines

PI: Metric analysis

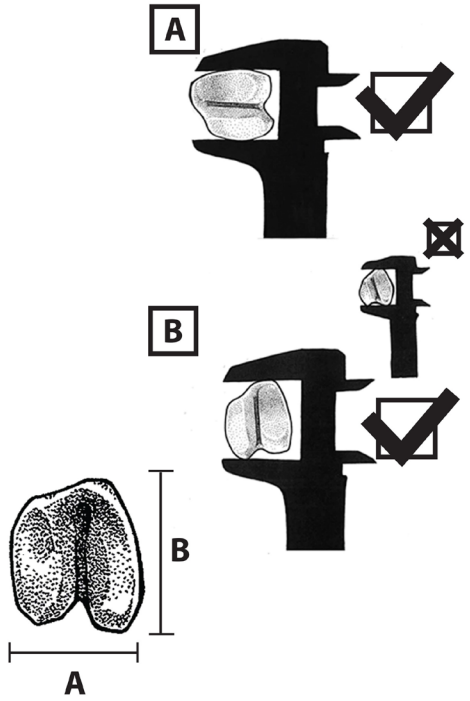

Measuring instructions

A: Measure the widest breadth of the phalanx.

B: Measure the longest length of the base of the phalanx, making sure that the central groove is parallel to the calipers. Do not lean the bone so that both dorsal protuberances rest against the calipers.

Note: Be sure that the measurement is taken from the edge of the articular surface not from the rugged area distal to it.

Equation: A/B = X

X ≥1= Thoracic (Fore)

X < 1= Pelvic (Hind)

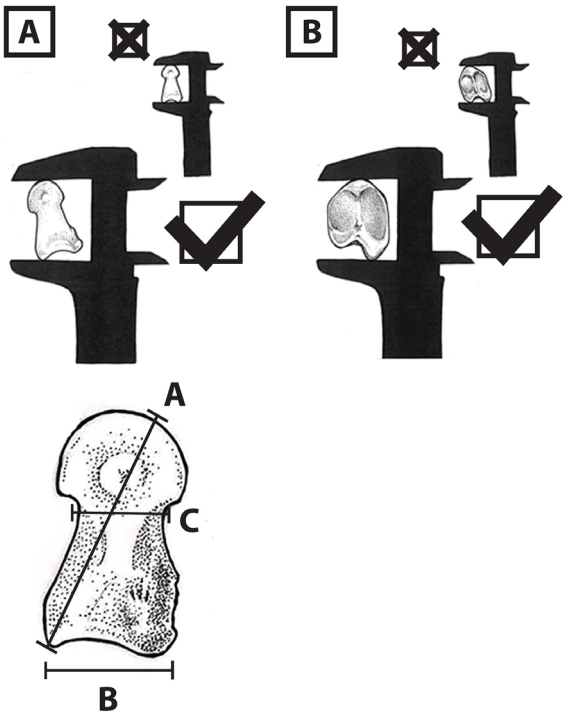

Measuring instructions

A: Measure the longest length from the head of the phalanx on the lateral side to the apex of the proximal ventral protuberance. Measure from the highest point on the head. Once correctly positioned, the phalanx may rotate freely between measurement points in the calipers. This is a sign that the phalanx is in the correct measurement position.

B: Measure the longest length of the base of the phalanx, making sure that the central ridge is parallel to the calipers. Do not lean the bone so that both dorsal protuberances rest against the calipers. To ensure this, identify the small, flat ovoid surface on the proximal dorsal aspect of the phalanx and rest this flat area flush against the calipers during measurement.

C: Measure the narrowest area of constriction on the neck of the phalanx, from the side of the phalanx, measuring from the dorsal to ventral surfaces, not side to side.

Equation: (A+B)/C = X

Round your results to the nearest hundredth, e.g. 4.01.

X < 4.50: Thoracic (Fore)

X > 4.50: Pelvic (Hind)

X = 4.50: Please re-check your measurements. If you still get 4.50, this bone must be marked as "undetermined".